J. Fluid Mech. (1973), *vol.* 58, *part* 2, *pp.* 233–261
Printed in Great Britain

Spectral transfer of scalar and velocity fields in heated-grid turbulence

By T. T. YEH AND C. W. VAN ATTA

Institute for Pure and Applied Physical Sciences and Department of Applied Mechanics and Engineering Science, University of California, San Diego

(Received 22 March 1972 and in revised form 27 October 1972)

For locally isotropic, homogeneous fluid turbulence, a digital Fourier analysis method of measuring directly the net scalar and velocity spectral transfer $T_n(k)$ of scalar and kinetic energy to a particular wavenumber from all other wavenumbers is described and applied to heated-grid turbulence. The technique uses the imaginary part of a particular cross-spectrum to obtain the one-dimensional net spectral transfer function $L_n(k_1)$ of velocity and scalar turbulence, and is a refinement of that used previously by Van Atta & Chen for measuring the velocity kinetic energy transfer.

The detailed spectral transfer $T_n(k, k')$ from one wavenumber to any other is related to the imaginary part of a particular three-dimensional bispectrum. $T_n(k, k')$ can be, in principle, computed from a particular two-dimensional triple correlation. Unlike $T_n(k)$, which can be obtained from $L_n(k_1)$, $T_n(k, k')$ cannot be determined from the measurable one-dimensional bispectrum $B_{1,n,n}(k_1, k_1')$ nor the one-dimensional transfer spectrum $L_n(k_1, k_1')$.

The measured net transfer spectra $T_n(k)$ have been used to determine the extent of validity for heated-grid turbulence of the dynamical equations for the three-dimensional power spectra of temperature and velocity in locally isotropic turbulence. The measured temperature transfer spectrum is also compared with those obtained from the power spectra of velocity and temperature by using various simple hypotheses.

1. Introduction

We consider here a locally isotropic, passive temperature field coupled with a locally isotropic velocity field, which may be approximately realized by introducing a heated grid into a uniform flow. At a sufficient distance downstream from the heated grid the temperature and velocity fields approach locally isotropic conditions (Kistler, O'Brien & Corrsin 1956; Mills, Kistler, O'Brien & Corrsin 1958). The present study is restricted to an incompressible fluid, and temperature fluctuations sufficiently small that the density is effectively constant, and buoyancy forces are negligible. Thus the thermal field does not influence the momentum equation and the scalar quantity is a passive tracer.

The determination of the transfer process between any arbitrary pair of wavenumbers produced by the nonlinear inertial forces is the central problem in understanding the decay of a homogeneous turbulent field. The original goal of

the present investigation was to carry out an experimental study of the three-dimensional bispectrum functions which describe the detailed balancing of the spectral transfer from one wavenumber to another. However, the present analysis indicates that available experimental techniques are not well suited for such a study, and the required measurements are sufficiently complex as to appear marginally desirable at present. Hence the present experiments consider only the much simpler problem of measurement of the net spectral transfer to a particular wavenumber from all other wavenumbers.

For velocity fluctuations alone, the kinetic energy transfer spectrum has been measured indirectly by Uberoi (1963) and both directly using triple correlations and also indirectly from the spectrum by Van Atta & Chen (1969) (here often referred to as I and II, respectively). In this study a conceptually different method of direct measurement of net scalar and velocity spectral transfer by using digital harmonic analysis was employed. The method uses the imaginary parts of certain cross-spectra, which correspond to one-dimensional integrals of one-dimensional bispectra of velocity and scalar fluctuations.

2. Basic equations

The derivations which follow are based on those found in Batchelor (1953), Hinze (1959) and Monin & Yaglom (1967). The governing equations describing the fluid motion and the distribution of temperature in an incompressible flow are

$$\left.\begin{aligned} \partial u_i/\partial x_i &= 0, \\ \frac{\partial u_i}{\partial t}+u_j\frac{\partial u_i}{\partial x_j} &= -\frac{1}{\rho}\frac{\partial p}{\partial x_i}+\nu\nabla^2 u_i, \\ \frac{\partial \theta}{\partial t}+u_j\frac{\partial \theta}{\partial x_j} &= \nu_\theta\nabla^2\theta, \end{aligned}\right\} \tag{1}$$

where $u_i(\mathbf{x})$ $(i = 1, 2, 3)$ and $\theta(\mathbf{x})$ are the velocity and temperature fluctuations, respectively; ν and ν_θ are the kinematic viscosity and the coefficient of molecular diffusion of temperature, respectively.

After taking the Fourier transform of (1) and using the incompressibility condition to eliminate the pressure we have

$$\left.\begin{aligned} k_i F_i(\mathbf{k}) &= 0, \\ \frac{\partial}{\partial t}F_i(\mathbf{k}) &= -ik_j\iiint F_j(\mathbf{k}-\mathbf{k}')\left[F_i(\mathbf{k}')-\frac{k_i k_l}{k^2}F_l(\mathbf{k}')\right]d\mathbf{k}'-\nu k^2 F_i(\mathbf{k}), \\ \frac{\partial}{\partial t}F_\theta(\mathbf{k}) &= -ik_j\iiint F_j(\mathbf{k}-\mathbf{k}')\,F_\theta(\mathbf{k}')\,d\mathbf{k}'-\nu_\theta k^2 F_\theta(\mathbf{k}), \end{aligned}\right\} \tag{2}$$

where

$$F_n(\mathbf{k}) = F_n^*(-\mathbf{k}) = (2\pi)^{-3}\iiint u_n(\mathbf{x})\exp\{-i\mathbf{k}.\mathbf{x}\}\,d\mathbf{x}, \tag{3}$$

in which $n = 1, 2, 3$ or θ, with $u_\theta(\mathbf{x}) \equiv \theta(\mathbf{x})$, and * denotes the complex conjugate.

From (2), the spectral equations for turbulent velocity and for turbulent temperature fluctuations can be written in the same form as

$$\frac{\partial}{\partial t}[\tfrac{1}{2}\Phi_{n,n}(\mathbf{k})] = \iiint T_n(\mathbf{k},\mathbf{k}')\,d\mathbf{k}'-\nu_n\mathbf{k}^2\Phi_{n,n}(\mathbf{k}), \tag{4}$$

where
$$\Phi_{n,n}(\mathbf{k}) = \Delta k^3 \langle F_n^*(\mathbf{k})\, F_n(\mathbf{k})\rangle \tag{5}$$

are the three-dimensional power spectra and

$$T_n(\mathbf{k},\mathbf{k}') = \tfrac{1}{2} i(\Delta k)^3 k_l \langle F_l^*(\mathbf{k}-\mathbf{k}')\, F_n^*(\mathbf{k}')\, F_n(\mathbf{k}) - F_l(\mathbf{k}-\mathbf{k}')\, F_n^*(\mathbf{k})\, F_n(\mathbf{k}')\rangle, \tag{6}$$

where Δk is the wavenumber increment in the discrete Fourier transform. The subscript n refers to quantities for either the velocity field or the temperature field. The repetition of the index n indicates summation, e.g.

$$\Phi_{n,n} \equiv \Phi_{i,i} \equiv \Phi_{1,1} + \Phi_{2,2} + \Phi_{3,3}$$

for velocity, while it is fixed (e.g. $\Phi_{n,n} \equiv \Phi_{\theta,\theta}$) and not summed for the temperature field. This notation will be used throughout this paper.

Thus, from (4), the $T_n(\mathbf{k},\mathbf{k}')$ may be interpreted (see, for example, Batchelor 1953, equation 5.2.7) as the net rates of spectral transfer from the volume element $d\mathbf{k}'$ to the element $d\mathbf{k}$ in wavenumber space. These spectral transfer functions are due to the inertial forces without regard to the pressure fluctuations. They satisfy a conservation law, since they are antisymmetric with respect to $\mathbf{k}$ and $\mathbf{k}'$, i.e. $T_n(\mathbf{k},\mathbf{k}') = -T_n(\mathbf{k}',\mathbf{k})$.

The double correlations are defined as

$$R_{n,m}(\mathbf{r}) = \langle u_n(\mathbf{x})\, u_m(\mathbf{x}+\mathbf{r})\rangle \tag{7}$$

and the three-point triple correlations as

$$R_{l,m,n}(\mathbf{r},\mathbf{r}') = \langle u_l(\mathbf{x})\, u_n(\mathbf{x}+\mathbf{r})\, u_m(\mathbf{x}+\mathbf{r}')\rangle. \tag{8}$$

Their Fourier transforms, with the aid of the convolution theorem, can be expressed as

$$\Phi_{n,m}(\mathbf{k}) = (2\pi)^{-3} \iiint R_{n,m}(\mathbf{r}) \exp\{-i\mathbf{k}.\mathbf{r}\}\, d\mathbf{r} = (\Delta k)^3 \langle F_n^*(\mathbf{k})\, F_m(\mathbf{k})\rangle, \tag{9}$$

where $\Phi_{n,m}$ is called the three-dimensional energy spectrum tensor, which reduces to (5) if $n = m$; and

$$\begin{aligned} B_{l,n,m}(\mathbf{k},\mathbf{k}') &= (2\pi)^{-6} \iiiint\!\!\iiint R_{l,n,m}(\mathbf{r},\mathbf{r}') \exp\{-i(\mathbf{k}.\mathbf{r}+\mathbf{k}'.\mathbf{r}')\}\, d\mathbf{r}\, d\mathbf{r}' \\ &= \Delta k^3 \langle F_l(\mathbf{k}'')\, F_m(\mathbf{k}')\, F_n(\mathbf{k})\rangle, \quad \text{with} \quad \mathbf{k}+\mathbf{k}'+\mathbf{k}'' = 0. \end{aligned} \tag{10}$$

$B_{l,n,m}$ is called the three-dimensional bispectrum and represents the spectral contributions to the three-point third-order correlation of a random variable from the product of three Fourier components whose resultant wavenumber is zero. The symmetry properties of the bispectrum for $n = m$ are obtained immediately from (10):

$$\begin{aligned} B_{l,n,n}(\mathbf{k},\mathbf{k}') &= B_{l,n,n}^*(-\mathbf{k},-\mathbf{k}') = B_{l,n,n}(\mathbf{k}',\mathbf{k}) \\ &= B_{n,l,n}(\mathbf{k}'',\mathbf{k}) = B_{n,l,n}(\mathbf{k}'',\mathbf{k}') \\ &= B_{n,n,l}(\mathbf{k},\mathbf{k}'') = B_{n,n,l}(\mathbf{k}',\mathbf{k}''). \end{aligned} \tag{11}$$

The main motivation for studying the bispectrum of turbulence would thus be to investigate certain nonlinear properties such as spectral energy transfer.

In general, the bispectrum does not necessarily indicate a nonlinear effect in

an inhomogeneous random field. Inhomogeneity implies phase consistency between pairs of wavenumbers, and this leads to phase consistency between triplets, which produces a non-vanishing bispectrum. Grid-generated turbulence is considered to be locally homogeneous and near Gaussian. Small but crucial deviations from normality exist because of the nonlinearities in the equations of motion. These can be determined to the first order by measuring the bispectrum or the spectral transfer. We note that several investigators, Brillinger (1965), Rosenblatt & Van Ness (1965) and Haubrich (1965), have studied one-dimensional bispectra of various stochastic variables both theoretically and experimentally.

After the expression for the bispectrum, equation (10), has been substituted into (6), the transfer spectrum function $T_n(\mathbf{k}, \mathbf{k}')$ can be expressed as

$$\begin{aligned} T_n(\mathbf{k}, \mathbf{k}') &= \tfrac{1}{2} ik_l [B_{l,n,n}(\mathbf{k}, -\mathbf{k}') - B^*_{l,n,n}(\mathbf{k}, -\mathbf{k}')] \\ &= -k_l \operatorname{Im} [B_{l,n,n}(\mathbf{k}, -\mathbf{k}')], \end{aligned} \tag{12}$$

where Im denotes the imaginary part. Thus, measurements of the bispectrum give the spectral energy transfer from one particular wavenumber to another wavenumber. The transfer function $T_n(\mathbf{k}, \mathbf{k}')$ depends only on the imaginary part of the bispectrum $B_{l,n,m}(\mathbf{k}, \mathbf{k}')$.

For an isotropic field, the bispectrum $B_{l,n,n}$ is a purely imaginary quantity; thus (12) reduces to

$$T_n(\mathbf{k}, \mathbf{k}') = ik_l B_{l,n,n}(\mathbf{k}, -\mathbf{k}'). \tag{13}$$

Therefore, if the three-point triple correlation $R_{l,n,n}(\mathbf{r}, \mathbf{r}')$ or the corresponding bispectrum $B_{l,n,n}(\mathbf{k}, \mathbf{k}')$ is known, the detailed balancing of the three-dimensional wavenumber transfer spectrum $T_n(\mathbf{k}, \mathbf{k}')$ from one wavenumber to another in the turbulent field is known.

3. Symmetry conditions and possible measurements

Although the full three-dimensional wavenumber expressions are of basic interest, no known way exists to make direct measurements of the necessary quantities. With the aid of Taylor's hypothesis of a 'frozen' turbulent structure (Lin 1953; Lumley 1965; Comte-Bellot & Corrsin 1971) the experimenter can make a Fourier analysis with respect to one space co-ordinate only. The three-dimensional form may be reduced to simpler forms by applying the isotropic symmetry conditions to see whether they become simple enough for laboratory measurement.

From Batchelor (1953) or Hinze (1959), the three-dimensional power spectrum $E_n(k)$ in terms of the one-dimensional power spectrum is

$$\begin{aligned} E_n(k) &= \int \tfrac{1}{2} \Phi_{n,n}(\mathbf{k})\, d\Omega_k = 2\pi k^2 \Phi_{n,n}(\mathbf{k}) \\ &= -k\, d\phi_{nn}(k)/dk, \end{aligned} \tag{14}$$

where $d\Omega_k$ denotes an integration over all solid angles while keeping a fixed value of k.

The quantity

$$\begin{aligned}\phi_{nn}(k_1) &= \int\int \Phi_{n,n}(\mathbf{k})\, dk_2\, dk_3 \\ &= (2\pi)^{-1}\int R_{n,n}(r_1)\exp\{-ik_1r_1\}\, dr_1 \\ &= \Delta k\langle U_n^*(k_1)\, U_n(k_1)\rangle \end{aligned} \tag{15}$$

is the one-dimensional power spectrum;

$$\begin{aligned}U_n(k_1) &= \int\int F_n(\mathbf{k})\, dk_2\, dk_3 \\ &= \frac{1}{2\pi}\int u_n(x_1, 0, 0)\exp\{-ik_1x_1\}\, dx_1 \quad (n = 1, 2, 3, \text{ or } \theta)\end{aligned} \tag{16}$$

is a one-dimensional Fourier transform of $u_n(x)$. Thus, (14) and (15) give

$$\int_0^\infty E_n(k)\, dk = \int_0^\infty \phi_{nn}(k_1)\, dk_1 = \tfrac{1}{2}\langle u_n u_n\rangle \tag{17}$$

and the three-dimensional dissipation spectrum

$$D_n(k) = \int \nu_n k^2 \Phi_{n,n}(\mathbf{k})\, d\Omega_k = 2\nu_n k^2 E_n(k). \tag{18}$$

Following Robertson (1940) or Batchelor (1953), and using the incompressibility condition, the first-order isotropic tensor $B_{l,n,n}(\mathbf{k}, \mathbf{k}')$ involving two vector variables can be written in general as

$$B_{l,n,n}(\mathbf{k}, \mathbf{k}') = A_n(k, \mu_k, k')\,[(k'^2 + kk'\mu_k)\, k_l - (k^2 + kk'\mu_k)\, k'_l], \tag{19}$$

where $A_n(k, \mu_k, k') = -A_n(k', \mu_k, k)$ and $\mu_k = \mathbf{k}.\mathbf{k}'/kk'$.

Thus from (13)

$$\begin{aligned}T_n(k, k') &= \int\int T_n(\mathbf{k}, -\mathbf{k}')\, d\Omega_k\, d\Omega_{k'} \\ &= i8\pi^2 k^4 k'^4 \int_{-1}^{1} A_n(k, \mu_k, k')\,(1 - \mu_k^2)\, d\mu_k \\ &= i8\pi^2 k^4 k'^4 \bar{A}_n(k, k').\end{aligned} \tag{20}$$

The following discussion indicates what kind of information about the spectral transfer may or may not be obtained experimentally.

One-dimensional bispectrum $B_{1,n,n}(k_1, k'_1)$

A one-dimensional bispectrum $B_{1,n,n}(k_1, k'_1)$ may be defined by integration of the three-dimensional bispectrum $B_{1,n,n}(\mathbf{k}, \mathbf{k}')$ over all values of the lateral components of wavenumber, k_2 and k_3, from (10):

$$\begin{aligned}B_{1,n,n}(k_1, k'_1) &= \int\int\int\int B_{1,n,n}(\mathbf{k}, \mathbf{k}')\, dk_2\, dk_3\, dk'_2\, dk'_3 \\ &= (2\pi)^{-2}\int\int R_{1,n,n}(r_1, 0, 0; r'_1, 0, 0)\exp\{-i(k_1r_1 + k'_1r'_1)\}\, dr_1\, dr'_1 \\ &= \Delta k\langle U_1(k''_1)\, U_n(k'_1)\, U_n(k_1)\rangle, \quad \text{with} \quad k_1 + k'_1 + k''_1 = 0.\end{aligned} \tag{21}$$

The one-dimensional bispectrum can be easily obtained and, from it, the co-linear three-point triple correlation $R_{1,n,n}(r_1, 0, 0; r_1', 0, 0)$ can be determined. In a study of multi-point velocity correlations, Van Atta & Yeh (1970) adopted a modified but similar method to calculate these correlations.

Substitution of (19) into (21) yields

$$B_{1,n,n}(k_1, k_1') = \iiint\int A_n(k, \mu_k, k')\,[(k'^2 + kk'\mu_k)\,k_1 - (k^2 + kk'\mu_k)\,k_1']\,dk_2\,dk_3\,dk_2'\,dk_3'$$

$$= 4\pi \int_{k_1}^{\infty} k^2\,dk \int_{k_1'}^{\infty} k'^2\,dk' \int_{\mu_-}^{\mu_+} f_n(k, \mu_k, k'; k_1, k_1')\,d\mu_k, \tag{22}$$

$$\mu_\pm = \{k_1 k_1' \pm [(k^2 - k_1^2)\,(k'^2 - k_1'^2)]^{\frac{1}{2}}\}/kk'$$

and

$$f_n(k, \mu_k, k'; k_1, k_1') = A_n(k, \mu_k, k')\,[(k'^2 + kk'\mu_k)\,k_1 - (k^2 + kk'\mu_k)\,k_1']$$

$$\times\,[k^2 k'^2(1-\mu_k^2) - (k_1 k' - kk_1')^2 - 2k_1 k_1' kk'(1-\mu_k)]^{-\frac{1}{2}}, \tag{23}$$

in which the isotropic conditions have been employed.

The one-dimensional bispectrum $B_{1,n,n}(k_1, k_1')$ gives only integral information about the three-dimensional bispectrum, which is insufficient to determine the function $A_n(k, \mu_k, k')$, or its angular integral $\bar{A}_n(k, k')$. Consequently, it is not possible to determine the transfer function $T_n(k, k')$ from the one-dimensional bispectrum. The one-dimensional bispectrum of $u_n(t)$ completely specifies the three-point collinear triple correlation, so that there is, in principle, no more information obtainable from single-probe measurements which could be used to calculate $T_n(k, k')$.

Three-point triple correlations in two-dimensional space

The general form of the first-order isotropic tensor $R_{1,n,n}(\mathbf{r}, \mathbf{r}')$ involving two symmetric vector variables (Robertson 1940; Batchelor 1953) can be written as

$$R_{l,n,n}(\mathbf{r}, \mathbf{r}') = R_n(r, \mu_r, r')\,r_l + R_n(r', \mu_r, r)\,r_l', \tag{24}$$

where $\mu_r = \mathbf{r}.\mathbf{r}'/rr'$, from which

$$R_{2,n,n}(r_1; r_1', r_2') = R_{2,n,n}(r; r', \mu_r) = R_n(r', \mu_r, r)\,r'(1-\mu_r^2)^{\frac{1}{2}}$$

or

$$R_n(r', \mu_r, r) = R_{2,n,n}(r; r', \mu_r)\,(r'(1-\mu_r^2)^{\frac{1}{2}})^{-1} \quad \text{for} \quad \mu_r^2 \neq 1. \tag{25}$$

After substitution of (25) into (24), the triple correlation in the full three-dimensional space becomes

$$R_{l,n,n}(\mathbf{r}, \mathbf{r}') = (1-\mu_r^2)^{-\frac{1}{2}} \left[\frac{r_l}{r} R_{2,n,n}(r'; r, \mu_r) + \frac{r_l'}{r'} R_{2,n,n}(r; r', \mu_r)\right] \quad \text{for} \quad \mu_r \neq 1,$$

$$= \cos(l, r)\,R_{1,n,n}(r, r') \quad \text{for} \quad \mu_r = 1, \tag{26}$$

where $\cos(l, r)$ is the direction cosine of the angle between the vector $\mathbf{r}$ and the x_l axis.

From the above, the transfer spectrum $T_n(k, k')$ may be obtained, but the measurement of two-dimensional triple correlations is a task of considerable magnitude; in fact, the measurement of $R_{2,n,n}(r; r', \mu_r)$ in an entire two-dimensional space would not only be difficult and laborious, but may also lead to problems of convergence for time series of reasonable length.

4. Net spectral transfer functions

As discussed in previous sections, the spectral transfer from dk' to dk cannot be determined from the one-dimensional bispectrum function, and its determination from two-dimensional triple correlations may not be practical. Here, the problem will be simplified to the net spectral transfer to dk from all other wavenumbers, that is,

$$T_n(\mathbf{k}) = \iiint T_n(\mathbf{k}, \mathbf{k}')\, d\mathbf{k}'. \tag{27}$$

The expression given for the transfer function $T_n(\mathbf{k}, \mathbf{k}')$ in (12) holds for any homogeneous flow, while equation (13) is good only for an isotropic field, in which the bispectrum function $B_{l,n,n}(\mathbf{k}, \mathbf{k}')$ is a pure imaginary number; i.e. the triple correlations $R_{l,n,n}(\mathbf{r}, \mathbf{r}')$ are purely antisymmetrical functions of $\mathbf{r}$ and $\mathbf{r}'$.

In actual grid-generated turbulence, the bispectral functions are found not to be purely imaginary quantities, so (12) instead of (13) should be used to express $T_n(\mathbf{k}, \mathbf{k}')$ in locally isotropic grid-generated turbulence; however, the isotropic conditions will be applied here to simplify the problem.

Thus, the net spectral transfer is

$$\begin{aligned} T_n(\mathbf{k}) &= -k_l \operatorname{Im}\left[\iiint B_{l,n,n}(\mathbf{k}, -\mathbf{k}')\, d\mathbf{k}'\right] \\ &= -k_l \operatorname{Im}\left[S_{ln,n}(\mathbf{k})\right], \end{aligned} \tag{28}$$

in which a new function, the cross-spectrum $S_{ln,n}(\mathbf{k})$, is defined. From (10)

$$S_{ln,n}(\mathbf{k}) = \iiint B_{l,n,n}(\mathbf{k}, -\mathbf{k}')\, d\mathbf{k}' \tag{29a}$$

$$= \frac{1}{(2\pi)^3} \iiint R_{l,n,n}(\mathbf{r}, 0) \exp\{-i\mathbf{k}.\mathbf{r}\}\, d\mathbf{r} \tag{29b}$$

$$= S_n(k)\, k_l. \tag{29c}$$

The last expression incorporates the isotropic condition for the cross-spectrum $S_{ln,n}(\mathbf{k})$, a first-order single-variable tensor.

Again, a one-dimensional cross-spectrum $S_{1n,n}(k_1)$ may be defined by integrating the three-dimensional cross-spectrum $S_{1n,n}(\mathbf{k})$ over all k_2 and k_3. From (29), $S_{1n,n}(k_1)$ can be expressed in several different (but equivalent) ways as follows:

$$S_{1n,n}(k_1) = \iint S_{1n,n}(\mathbf{k})\, dk_2\, dk_3 \tag{30}$$

$$= \int B_{1,n,n}(k_1, k_1')\, dk_1' \quad \text{from (29}a\text{) and (21)} \tag{30a}$$

$$= \frac{1}{2\pi} \int R_{1n,n}(r_1) \exp\{-ik_1 r_1\}\, dr_1 \quad \text{from} \quad (29b) \tag{30b}$$

$$= \Delta k \langle U_{1n}^*(k_1)\, U_n(k_1) \rangle \tag{30c}$$

$$= \iint S_n(k)\, k_1\, dk_2\, dk_3 \quad \text{from} \quad (29c) \tag{30d}$$

$$= k_1 \int_0^{2\pi} d\phi \int_0^{\infty} S_n(k)\, \sigma\, d\sigma$$

$$= 2\pi k_1 \int_{k_1}^{\infty} S_n(k)\, k\, dk. \tag{30e}$$

Equation (30*c*) is obtained from (30*b*) by using the convolution theorem, and defining a new basic measurable function similar to $U_n(k_1)$ in (16):

$$U_{1n}(k_1) = \frac{1}{2\pi} \int u_1(x)\, u_n(x) \exp\{-ik_1 x\}\, dx \quad (n = 1, 2, 3, \text{ or } \theta), \tag{31}$$

and in passing from (30*d*) to (30*e*) we have used cylindrical co-ordinates, i.e.

$$(k_1, k_2, k_3) \to (k_1, \sigma, \phi), \quad \text{with} \quad k^2 = k_1^2 + \sigma^2 = k_1^2 + k_2^2 + k_3^2.$$

From (30*e*) $$S_n(k) = \frac{1}{2\pi k^3} \left(S_{1n,n}(k) - k \frac{d}{dk} S_{1n,n}(k) \right). \tag{32}$$

Therefore, from (28), (29*c*) and (32),

$$T_n(\mathbf{k}) = -k^2 \operatorname{Im}[S_n(k)]$$

$$= \frac{-1}{2\pi k} \left\{ \operatorname{Im}[S_{1n,n}(k)] - k \frac{d}{dk} \operatorname{Im}[S_{1n,n}(k)] \right\} \tag{33}$$

and thus

$$T_n(k) = \int T_n(\mathbf{k})\, d\Omega_k = 4\pi k^2 T_n(\mathbf{k})$$

$$= -2k \left\{ \operatorname{Im}[S_{1n,n}(k)] - k \frac{d}{dk} \operatorname{Im}[S_{1n,n}(k)] \right\}$$

$$= 4L_n(k) - 2k\, dL_n(k)/dk, \tag{34}$$

where $L_n(k) = -k \operatorname{Im}[S_{1n,n}(k)]$ may be defined as the total one-dimensional spectral energy transfer.

The cross-spectrum $S_{1n,n}(k)$, which plays the role of a measurable transfer function, can be obtained in several ways: (*a*) from (30*a*) by integration of the one-dimensional bispectrum (Brillinger 1965; Rosenblatt & Van Ness 1965; Haubrich 1965; Van Atta & Yeh 1970); (*b*) from (30*b*) by the Fourier transform of the two-point triple correlation $R_{1n,n}(r_1)$ [previously measured for the velocity field in grid turbulence by Townsend (1947), Stewart (1951), Stewart & Townsend (1951), Frenkiel & Klebanoff (1967) and Van Atta & Chen (1968), and for the mixed temperature–velocity field by Kistler *et al.* (1956) and Mills *et al.* (1958)]; or (*c*) from (30*c*) using the directly estimated cross-spectrum of

$$u_{1n}(x) = u_1(x)\, u_n(x) \quad \text{and} \quad u_n(x).$$

The last method is the most direct one for obtaining $S_{1n,n}(k_1)$ and was adopted in the present study to calculate the transfer function $T_n(k)$.

This method for obtaining $T_n(k)$, the spectral transfer functions for both velocity and temperature fields, is essentially the same as that reported in II by Van Atta & Chen for obtaining $T_u(k)$, the spectral transfer function for velocity kinetic energy. However, we have found a further justification for one of the steps and we have eliminated two unnecessary computational steps. In measuring

the transfer spectrum $T_u(k)$ for fluid kinetic energy, Van Atta & Chen replaced the approximately antisymmetrical measured triple correlation $R_{1i,i}(r_1)$ by an exactly antisymmetrical function, the composite triple correlation

$$\mathscr{R}_{1i,i}(r_1) = \tfrac{1}{2}[R_{1i,i}(r_1) - R_{1i,i}(-r_1)].$$

We have found a further justification for this step. The original form of the transfer function suggests that (12) instead of (13) should be adopted when the flow field is not exactly isotropic. This means that the composite triple correlation $\mathscr{R}_{1i,i}(r_1)$, instead of the triple correlation $R_{1i,i}(r_1)$, should be used when $T_u(k)$ is obtained from the measured triple correlation.

Because they were especially interested in the form of the triple correlations, Van Atta & Chen employed some unnecessary steps in obtaining $\mathrm{Im}\,(S_{1i,i}(k_1)]$, whereas we obtain $\mathrm{Im}\,[S_{1i,i}(k_1)]$ more directly in the present work. In using the digital harmonic method, Van Atta & Chen obtained the cross-spectrum $S_{1i,i}(k_1)$ (and therefore $\mathrm{Im}\,[S_{1i,i}(k_1)]$) first and then obtained the triple correlation $R_{1i,i}(r_1)$ by taking the inverse Fourier transform of $S_{1i,i}(k_1)$. They then formed the composite triple correlation $\mathscr{R}_{1i,i}(r_1)$, and finally took its Fourier transform to obtain $\tilde{S}_{1i,i}(k_1)$.

In fact, the final quantity $-i\tilde{S}_{1i,i}(k_1)$ obtained by Van Atta & Chen is the same as the first one, $\mathrm{Im}\,[S_{1i,i}(k_1)]$, which is immediately obtained in the first step given above. So it is possible, and perhaps desirable in some future applications, to skip the intervening steps.

Referring to (30*b*), the imaginary part $\mathrm{Im}\,[S_{1i,i}(k_1)]$ of the cross-spectrum can be expressed as follows:

$$\begin{aligned}\mathrm{Im}\,[S_{1i,i}(k_1)] &= -\tfrac{1}{2}i[S_{1i,i}(k_1) - S^*_{1i,i}(k_1)] \\ &= \frac{-i}{2}\left[\frac{1}{2\pi}\int_{-\infty}^{\infty} R_{1i,i}(r_1)\exp\{-ik_1r_1\}\,dr_1\right. \\ &\qquad\left. -\frac{1}{2\pi}\int_{-\infty}^{\infty} R_{1i,i}(r_1)\exp\{ik_1r_1\}\,dr_1\right] \\ &= \frac{-i}{2\pi}\int_{-\infty}^{\infty}\mathscr{R}_{1i,i}(r_1)\exp\{-ik_1r_1\}\,dr_1 = -i\tilde{S}_{1i,i}(k_1),\end{aligned}$$

where $\tilde{S}_{1i,i}(k_1)$ is an imaginary number.

The spectral functions discussed in the previous sections apply to both turbulent velocity and scalar variations. The formulation presented for three-dimensional spectral functions requires the measurement of two time series simultaneously, namely, $u(t)$ and $v(t)$ for velocity fluctuations and $u(t)$ and $\theta(t)$ for scalar fluctuations. However, in the present investigation, the passive scalar fluctuations were of primary interest, and only two signals, $u(t)$ and $\theta(t)$, were measured. Thus, some functions, such as $\phi_{22}(k_1)$ and $S_{12,2}(k_1)$, which involve the lateral component of velocity v were not obtained directly. To obtain the three-dimensional spectra $E_u(k)$ and $T_u(k)$ for turbulent kinetic energy the one-dimensional spectra $\phi_{22}(k_1)$ and $S_{12,2}(k_1)$ were obtained from the measured $\phi_{11}(k_1)$ and $S_{11,1}(k_1)$ respectively by using the isotropic conditions (Batchelor 1953; Hinze 1959):

$$\phi_{22}(k_1) = \tfrac{1}{2}[\phi_{11}(k_1) - k_1\,d\phi_{11}(k_1)/dk_1] \tag{35}$$

and

$$S_{12,2}(k_1) = \tfrac{1}{4}[S_{11,1}(k_1) - k_1\,dS_{11,1}(k_1)/dk_1]. \tag{36}$$

5. Experimental arrangement

The experiments were carried out in the 76 cm by 76 cm by 9 m test section of the low-turbulence wind tunnel in the Department of Applied Mechanics and Engineering Sciences. As in the experiments of Kistler *et al.* (1956) and of Mills *et al.* (1958), the velocity and temperature fluctuations were simultaneously generated by a heated grid, which in the present case was located 2·44 m from the end of the contraction section. The square-mesh biplane heated grid was composed of 36 stainless sheath calrod tubular heaters, model 5D74, manufactured by General Electric. The grid mesh size M was 4 cm, with rods of diameter 8 mm. A vertical array of 18 thermistors on a horizontal traverse was used to measure the local mean temperature profile across the test section. These signals were fed into the heated-grid power control box, consisting of nine individual control circuits, to act as a feedback system. This automatically maintained a desired flat mean temperature profile, and was used for the hot-wire and cold-wire calibrations. The circuit could also be controlled manually to maintain a fixed power supply to the grid. This manual operation was used for the turbulence measurements, since a constant power input is required to maintain the constant temperature rise across the grid needed for generating stationary temperature fluctuations.

The power source for the heated grid was a 120 V, three-phase, 60 c/s alternating current. Gated-controlled full-wave silicon triacs were used to control the power in a full-wave on–off manner. The average power supplied to the grid therefore depended on the ratio of the power-on and power-off intervals. The minimum power-off interval was $\frac{1}{60}$ s; however, because of the very large thermal inertia of the rods, no 120 c/s periodic temperature component was detectable. In the present case, the rods were all heated evenly; hence the thermal mesh size was equal to that of the momentum mesh size.

It was found that, near the grid, the outer tunnel-wall boundary-layer flows were heated by the walls. The wall temperature was higher than that of the fluid because of the radiation from the hot grid. Moderate radiation effects were also found in the readings of thermistors and thermometers for $x/M \leqslant 30$. Therefore the mean temperature was based on the reading at $x/M = 50$, where the radiation effects were negligible. Two thermometers were used to determine the mean temperature rise ΔT_G across the grid and were located about 60 mesh lengths upstream and downstream from the grid. We also observed that stratified flow was developed at low speeds when the tunnel was operated in the closed-loop condition. This was unsuitable for the present study of isotropic fluctuations. Although we could maintain a uniform mean temperature profile at the test section by heating more in the lower rods, this clearly created non-uniform temperature fluctuations in the vertical direction, which was again not acceptable for this study.

To avoid this problem, the wind tunnel was operated in an open-loop manner. This was done by removing the last test section and replacing it by a piece of plywood connected to the tunnel floor at about a 30° vertical angle with respect to the axis of the test section or the mean flow direction. The heated air was

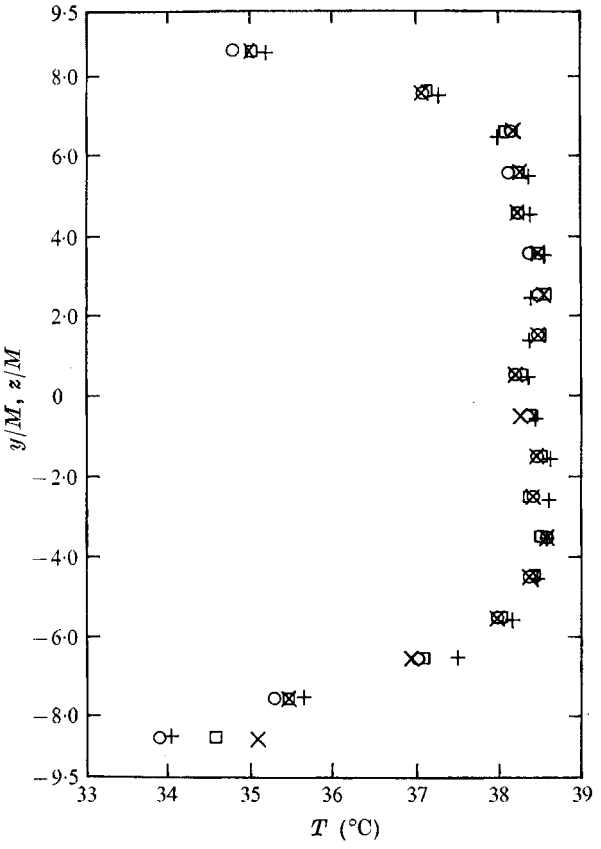

FIGURE 1. Mean temperature profiles across the tunnel. Horizontal: +, $x/M = 35$. Vertical: ○, $x/M = 35$; □, $x/M = 40$; ×, $x/M = 46{\cdot}6$.

deflected into the upper portion of the room and was eventually removed by the air-conditioning of the building, while colder air was sucked from the lower part of the room into the wind-tunnel intake.

The mean flow velocity U was about 4·06 m/s. The Reynolds number R_M based on M and U was about 10500 and the corresponding Péclet number $Pe_M = PrR_M$ was about 7650; $Pr = 0{\cdot}725$ for the working fluid, air. The temperature rise across the grid was about 10 °C, and the mean temperature was about 38 °C. The mean temperature was increased slowly during a run because of the temperature rise in the room (about 1·5 °C in 2 h). The mean temperature distribution across the tunnel is shown in figure 1.

The signal detection was complicated by the addition of temperature fluctuations to the usual velocity fluctuations (Corrsin 1947, 1949; Corrsin & Uberoi 1951). It was not practical to use the hot wire to measure velocity fluctuations alone in the present case because of the limitations on the hot-wire temperature. The simultaneously recorded hot- and cold-wire signals were used to calculate the true velocity and temperature fluctuations. A very small platinum wire, 0·25 μm in diameter and 1 mm long, with a resistance of about 1·3 kΩ was

operated as a resistance thermometer (cold wire). A modified Tektronix Q-type, a.c. strain gauge bridge (see, for example, Gibson & Schwarz (1963)) with a carrier frequency of 25 kHz and a bandwidth up to about 6 kHz was used to operate the cold wire. The overall frequency response of the thermometer was determined, using the method of Kidron (1966), by heating the cold wire with X-band microwaves and was found to be flat up to about 5 kHz. A very small heating current of about 50 μA was used to minimize the error due to velocity fluctuations. The bridge was balanced as close to zero as possible and the calibration was accomplished by varying the power into the heated grid. This calibration provided δ_2 in the relation

$$e_2 = \delta_2 \theta, \tag{37}$$

where e_2 is the output voltage fluctuation, δ_2 is the calibration constant and θ is the temperature fluctuation.

Both the temperature signal obtained by the cold wire and a mixed velocity–temperature signal, which was obtained from the hot-wire anemometer, were used to compute the longitudinal fluctuating component u of the velocity field at nearly the same spatial location as the measured temperature fluctuations. The cold wire was parallel to and about 0·5 mm below the hot wire, and was outside the thermal wake of the hot wire at all times. The hot wire, here called the velocity wire, was standard 10 % rhodium and 90 % platinum, 5 μm in diameter, 1 mm long, and responded predominantly to velocity fluctuations. A DISA 55A01 amplifier was used to operate the hot wire at constant resistance, with an overheat ratio of 0·6. The hot-wire response signal E_1 can be written in general form as $E_1^2 = f(\tilde{U}, \tilde{T})$, where $\tilde{U}$ and $\tilde{T}$ are the total velocity and temperature, respectively. For low intensities of velocity and temperature fluctuations, as in the present experiments, one may linearize the expression for the fluctuating voltage to obtain

$$e_1 = d(E_1^2) \cong E_1^2 - \langle E_1^2 \rangle \cong \beta_1(U,T)\, u + \delta_1(U,T)\, \theta, \tag{38}$$

where $$\beta_1(U,T) = [\partial E_1^2/\partial U]_{U,T}, \quad \delta_1(U,T) = [\partial E_1^2/\partial T]_{U,T}.$$

The calibrations were performed in the turbulent flow with temperature fluctuations, under the same mean conditions as those for which the turbulence measurements were made. The cold wire was calibrated over a range of a few degrees centigrade around $T = 38\,^{\circ}\mathrm{C}$ and $U = 4{\cdot}06$ m/s. The hot-wire calibration was much more laborious. The output calibration voltages for about 50 different conditions of U and T were measured and used to fit a surface in the least-squares-error sense:

$$E_1^2(U,T) = C_0 + C_1 U^{\frac{1}{2}} + C_2 T + C_3 U + C_4 U^{\frac{1}{2}} T + C_5 T^2, \tag{39}$$

where the C_i ($i = 0, \ldots, 5$) are the constants to be determined. The calibration constants are functions of the mean velocity U and the mean temperature T:

$$\beta_1(U,T) = C_3 + (C_1 + C_4 T)/2U^{\frac{1}{2}}$$

and

$$\delta_1(U,T) = C_2 + C_4 U^{\frac{1}{2}} + 2C_5 T.$$

For the turbulence measurements, the hot-wire and cold-wire signals were FM tape recorded simultaneously on magnetic tape at a tape speed of 76·2 cm/s using a Sanborn 3917A recorder. The analog tapes were later played back and

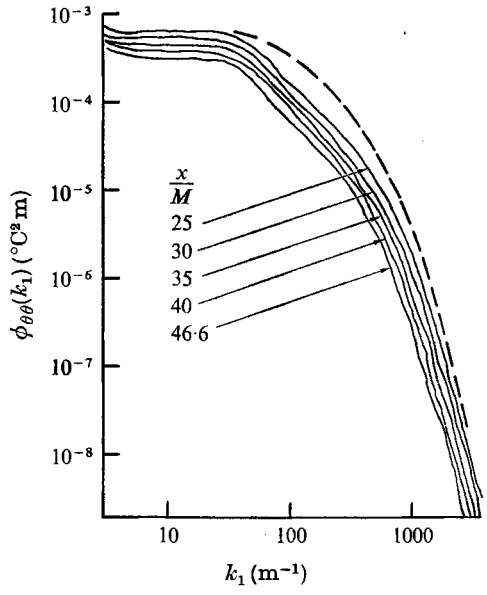

FIGURE 2. One-dimensional spectra of temperature fluctuations (computer plot). ———, data of Mills *et al.*, $x/M = 17$, arbitrary units.

the signals were band-passed (0·02 Hz–2 kHz) with Krohn–Hite filters, Model 3750. The high-pass filter was used to remove the undesired mean drift due to the slow mean temperature rise of the room. The highest frequency, 2 kHz, for which the temperature spectrum was unmistakably distinguishable from electronic noise was determined from a preliminary spectral analysis. The frequency $f^* \equiv v/2\pi l_K$ corresponding to the convection of the Kolmogorov microscale l_K past the probe at the mean flow speed was about 1·2 kHz. The band-passed signals were then sampled with an analog-to-digital converter at a rate of $f_s = 4170$ samples per second and recorded on digital tapes. The physical quantities u and θ were then computed from the sampled digital data and stored on another digital tape using a CDC 3600 computer. These last digital tapes were used later as input data for evaluating various quantities. A sampling interval of 73·5 s or 307 200 digital samples for both the hot-wire and cold-wire signals was found to be adequate to provide stationary values of the quantities calculated, and all subsequent averages were based on four samples of this length.

Many of the detailed measurements to be discussed were made in the initial region of decay at $x/M = 35$. For the determination of the spectral decay, measurements were made over a short range of x/M in the initial period of decay.

6. Experimental results *Energy spectra*

The one-dimensional energy spectra were directly calculated from the discrete Fourier transforms of the time series for instantaneous values of u and θ. The data were transformed in records each containing 2048 digital samples by using the fast Fourier algorithm method of Cooley & Tukey (1965). The measured

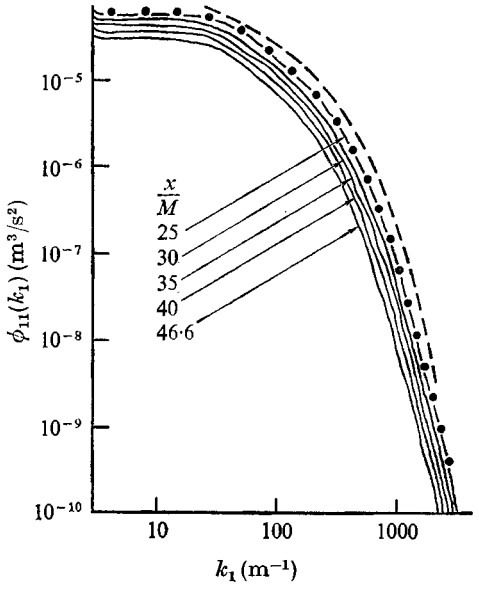

FIGURE 3. One-dimensional spectra of longitudinal velocity fluctuations (computer plot). ●, $x/M = 25$, with grid cold; ---, data of Mills *et al.*, $x/M = 17$, arbitrary units.

spectra for temperature and velocity are shown in figures 2 and 3, respectively, along with the spectra obtained by Mills *et al.*

Contrary to the results of Mills *et al.* (1958) the present measured temperature spectrum appears somewhat different from the measured velocity spectrum. The former has a roughly constant slope of about $-\frac{5}{3}$ for a short range of wave-numbers, while the latter does not. For the present small Reynolds number, the observed form of the temperature spectrum probably does not imply the existence of an inertial–convective subrange (Obukov 1949; Corrsin 1951; Batchelor 1959) and we have so far been able to give no satisfactory physical explanation for the appearance of the temperature spectrum.

To test the assumption that the temperature fluctuations were dynamically passive, both velocity-spectra and turbulence-level measurements were made with and without heating the grid. As shown in figures 3 and 7, both the resulting spectra and the turbulence levels are identical within experimental uncertainty. This result is consistent with the fact that the calculated ratio $\beta g\theta'\tau_f/u'$ of the r.m.s. gravitational buoyancy acceleration and the actual r.m.s. particle acceleration (Uberoi & Corrsin 1953) was very small (about $1{\cdot}5\times10^{-3}$), where g is the gravitational acceleration, β the coefficient of thermal expansion for air and τ_f the Lagrangian time microscale of the turbulent velocity. On the basis of the discussion of Batchelor (1967), the assumption that the velocity distribution is approximately solenoidal seems justified, because of the small values of

$$u'^2/a^2 \simeq 10^{-7}, \quad \beta u'/C_p R \simeq 10^{-9} \quad \text{and} \quad \beta\theta'/RPr = 10^{-5}$$

(a is the sound speed and Pr the Prandtl number).

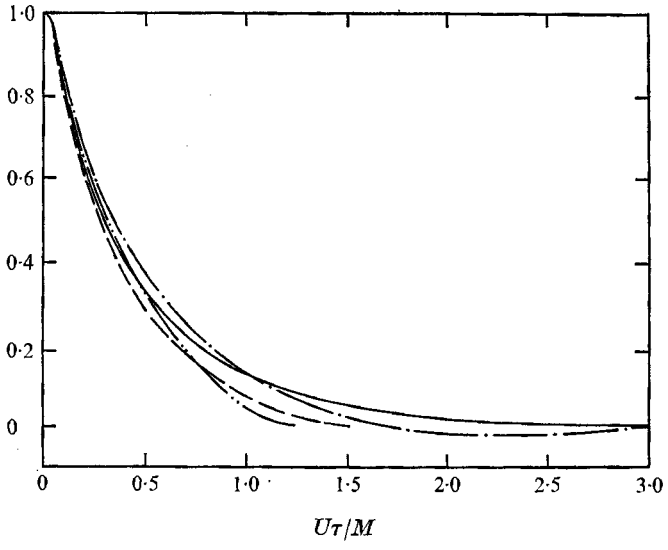

FIGURE 4. Comparison between $R(u,u)$ and $R(\theta,\theta)$ (computer plot). $R(u,u)$: ——, present results ($x/M = 35$); – – –, Mills *et al.* ($x/M = 17$). $R(\theta,\theta)$: —·—, present results ($x/M = 35$), —··—, Mills *et al.* ($x/M = 17$).

Figure 4 shows a typical comparison of the double correlations

$$R(u,u) = \langle u(t)\,u(t+\tau)\rangle/\langle u^2\rangle \quad \text{and} \quad R(\theta,\theta) = \langle \theta(t)\,\theta(t+\tau)\rangle/\langle \theta^2\rangle$$

at $x/M = 35$. Also shown is a similar comparison at $x/M = 17$ given by Mills *et al.* (1958). Our $R(\theta,\theta)$ is larger than $R(u,u)$ at small $U\tau/M$ and becomes smaller for $U\tau/M \geqslant 1{\cdot}0$. Similar behaviour is apparent in the data of Mills *et al.* However, the $R(\theta,\theta)$ obtained by them monotonically approaches a small positive value, whereas our $R(\theta,\theta)$ passes through zero at about $U\tau/M = 1{\cdot}6$, reaches a small negative maximum, and then returns to zero as $U\tau/M$ increases further.

Figure 5 shows the values of $\langle u\theta\rangle$ at five positions downstream from the grid. In contrast to the statement of Mills *et al.* that their $\langle u\theta\rangle$ was zero within the accuracy of their data, we find that, for $25 \leqslant x/M \leqslant 46{\cdot}6$, the measured cross-correlation $\langle u\theta\rangle/u'\theta'$ is of order $-0{\cdot}1$. The values of $\langle u\theta\rangle$ approach zero fairly slowly as x/M increases further downstream. These non-zero values of $\langle u\theta\rangle$ indicate the degree of overall anisotropy of the present flow. To resolve this anisotropy in terms of wavenumber and to determine if the temperature field may still satisfy the necessary (but not sufficient) condition $\langle u\theta\rangle_{k_1} = 0$ for local isotropy, the one-dimensional cross-spectrum of velocity and temperature was obtained from

$$\phi_{u\theta}(k_1) = \Delta k\langle U_u^*(k_1)\,U_\theta(k_1)\rangle = C_{u\theta}(k_1) + iQ_{u\theta}(k_1),$$

where $C_{u\theta}(k_1)$ and $Q_{u\theta}(k_1)$ are the co-spectrum and quadrature spectrum, respectively. The coherence A^2 and phase ϕ are given in terms of the spectra:

$$A^2(k_1) = |\phi_{u\theta}(k_1)|^2/\phi_{11}(k_1)\,\phi_{\theta\theta}(k_1) \quad \text{and} \quad \phi(k_1) = \tan^{-1}(Q_{u\theta}(k_1)/C_{u\theta}(k_1)).$$

The coherence plays the role of the cross-correlation of u and θ at each wavenumber. Both the coherence and the cross-correlation should be identically zero

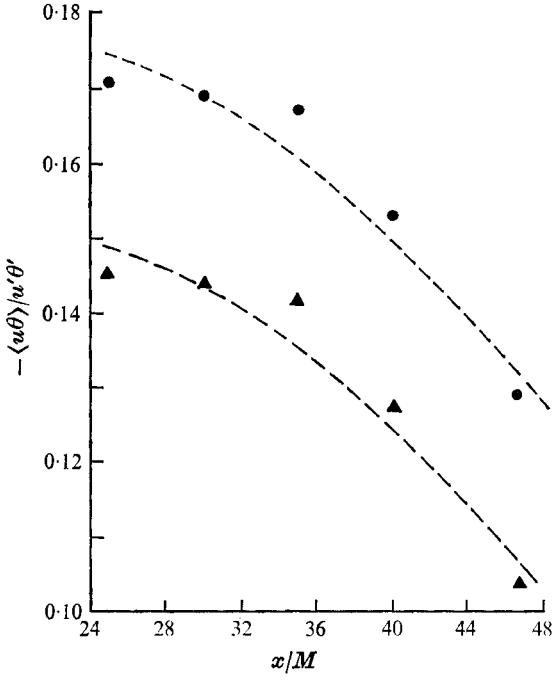

FIGURE 5. Cross-correlation between u and θ at several values of x/M. ●, $\langle u\theta\rangle/u'\theta'$, uncorrected measured value; ▲, $\langle u\theta\rangle_c/u'\theta'$ corrected for the velocity sensitivity of the cold wire; – – –, free-hand curve fit.

for all k_1 for strictly isotropic fluctuations (a stronger condition than local isotropy). The data in figure 6 show that large eddies are responsible for anisotropic contributions to $\langle u\theta\rangle$ and that the small eddies do not contribute to $\langle u\theta\rangle$. The negative correlation for small k_1 apparently indicates that the large eddies only very slowly forget their method of initial generation; i.e. one would expect negative correlation from the heated wakes of individual grid rods, in which the velocity is low and the temperature high relative to their mean values downstream.

The fluctuation intensities $\langle u^2\rangle$ and $\langle\theta^2\rangle$ obtained at five locations downstream from the heated grid are shown and compared with those of Mills *et al.* in figure 7. The decay rates of the velocity and temperature fluctuations are nearly the same for the present data. Similar behaviour was noted for the corresponding range of x/M by Mills *et al.*, who also noted that the decay rate of the temperature fluctuations decreased significantly relative to that of the velocity fluctuations for larger values of x/M than those considered in the present investigation. From these values the rates of dissipation $\epsilon_u = -\frac{3}{2}d\langle u^2\rangle/dt$ and $\epsilon_\theta = -\frac{1}{2}d\langle\theta^2\rangle/dt$ at $x/M = 35$ were calculated. These and other basic parameters of the flow conditions are given in table 1.

The three-dimensional energy spectra were determined from the measured one-dimensional spectra. Figures 8 and 9 show their absolute values at five x/M positions for temperature and velocity fluctuations, respectively. The eddy sizes $l_m = 1/k_m$ corresponding to spectral maxima and the integral scales L are shown in figure 10. The increase of l_m and L with x/M is due to the fact that

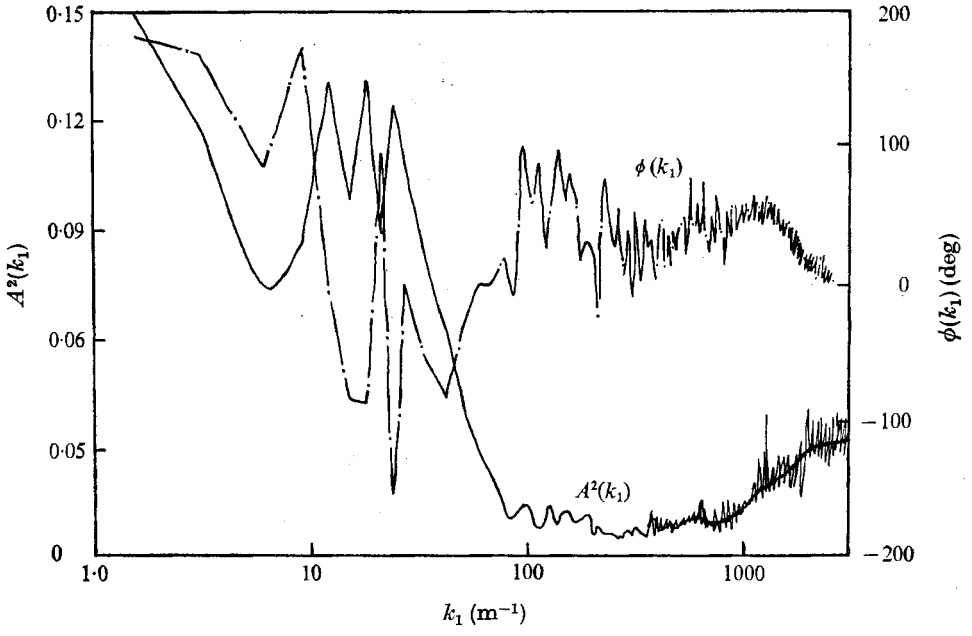

FIGURE 6. Coherence and phase difference of u and θ (computer plot). ——, $A^2(k_1)$; —·—, $\phi(k_1)$.

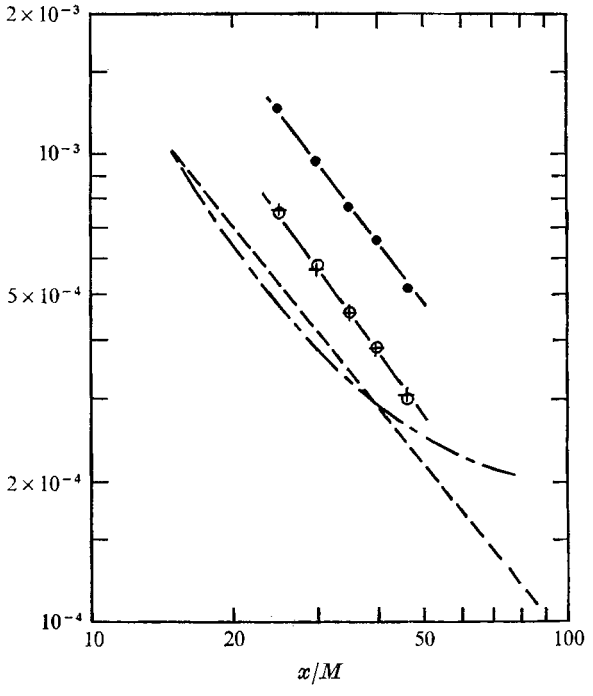

FIGURE 7. Decay of kinetic energy and temperature fluctuations downstream of the grid. $\langle u^2\rangle/U^2$: ○, present results, grid hot; +, present results, grid cold; – – –, Mills *et al.* $\langle\theta^2\rangle/\Delta T_G^2$: ●, present results; — — —, Mills *et al.*

Velocity		Temperature	
U	4·06 m/s	T	38·5 °C
M	4 cm	ΔT_G	10 °C
d	8 mm	$Pr = \nu/\nu_\theta$	0·725
$u' = \langle u^2\rangle^{\frac{1}{2}}$	0·08725 m/s	$\theta' = \langle\theta^2\rangle^{\frac{1}{2}}$	0·2776 °C
ν	$1{\cdot}55 \times 10^{-5}$ m^2/s	ν_θ	$2{\cdot}142 \times 10^{-5}$ m^2/s
ϵ_u	0·0456 m^2/s^3	ϵ_θ	0·154 °C^2/s
$k_k = (\epsilon_u/\nu^3)^{\frac{1}{4}}$	1872 m^{-1}	$k_B = Pr^{\frac{1}{2}} k_k$	1600 m^{-1}
$l_k = 1/k_k$	0·534 mm	$k_c = Pr^{\frac{3}{4}} k_k$	1475 m^{-1}
$\tau_k = (\nu/\epsilon_u)^{\frac{1}{2}}$	0·0187 s^{-1}	$l_B = 1/k_B$	0·625 mm
$v_k = (\epsilon_u \tau_k)^{\frac{1}{4}}$	0·0288 m/s	$\theta_k = (\epsilon_\theta \tau_k)^{\frac{1}{2}}$	0·0537 °C
$\lambda_f = (15\nu/\epsilon_u)^{\frac{1}{2}} u'$	6·25 mm	$\lambda_\theta = (6\nu_\theta/\epsilon_\theta)^{\frac{1}{2}} \theta'$	8·0 mm
$R_M = UM/\nu$	10 500	$Pe_M = UM/\nu_\theta$	7650
$R_\lambda = u'\lambda_f/\nu$	35·2	$Pe_{\lambda_\theta} = u'\lambda_\theta/\nu_\theta$	32·5
$K_1 = 9/55K_3$	0·22	$K_{\theta,1} = 3/5K_{\theta,3}$	0·38

TABLE 1. Basic parameters of the flow conditions for heated-grid turbulence at $x/M = 35$. The subscripts k, B and C refer to parameters associated with Kolmogorov, Batchelor and Corrsin, respectively. λ_f is the Taylor microscale; λ_θ is the Corrsin microscale.

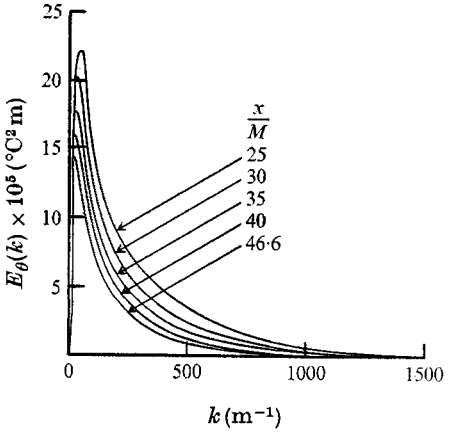

FIGURE 8. Three-dimensional spectra of temperature fluctuations.

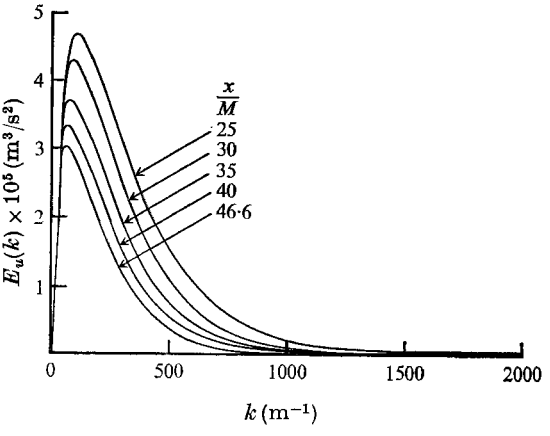

FIGURE 9. Three-dimensional spectra of kinetic energy.

the small eddies decay more rapidly than the large ones, although the small ones continually obtain energy from the large ones. As shown in figure 10, a similar slow increase of L with x/M was obtained by Mills *et al.* We find that l_m is larger for the temperature field than for the velocity field.

The normalized energy spectra and dissipation spectra are presented in figures 11 and 12. The normalizing parameters are defined in table 1. The values at high wavenumbers are too small to be shown in these figures. For large wavenumbers, the energy spectra are in good agreement with the measurements reported in I and II. There are large differences for small wavenumbers because of differences in turbulence intensities in the experiments, the inapplicability of the isotropic relations for such low wavenumbers, and the fact that Kolmogorov scaling is not expected to apply in this range. The values of k/k_k corresponding to

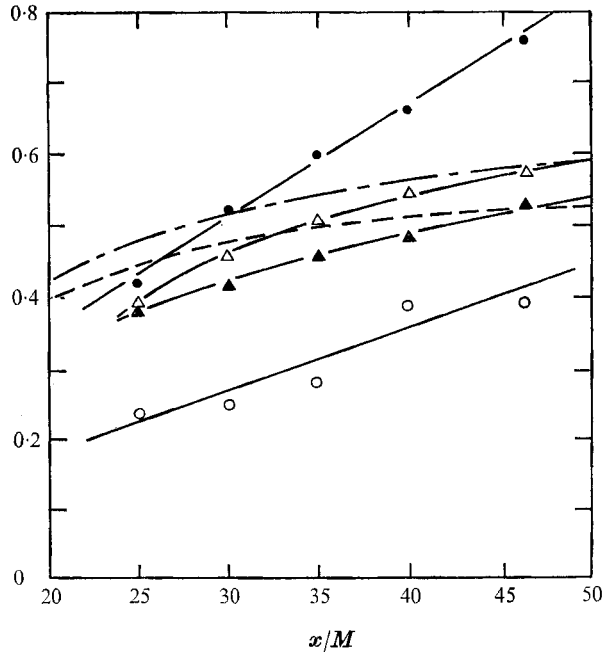

FIGURE 10. Eddy sizes l_m corresponding to spectral maxima and integral scales L for temperature and velocity fluctuations. Present results: ●, $l_{m,\theta}/M$; ○, $l_{m,u}/M$; ▲, L_θ/M; △, L_f/M. Mills *et al.*: – – –, L_θ/M; — · —, L_f/M.

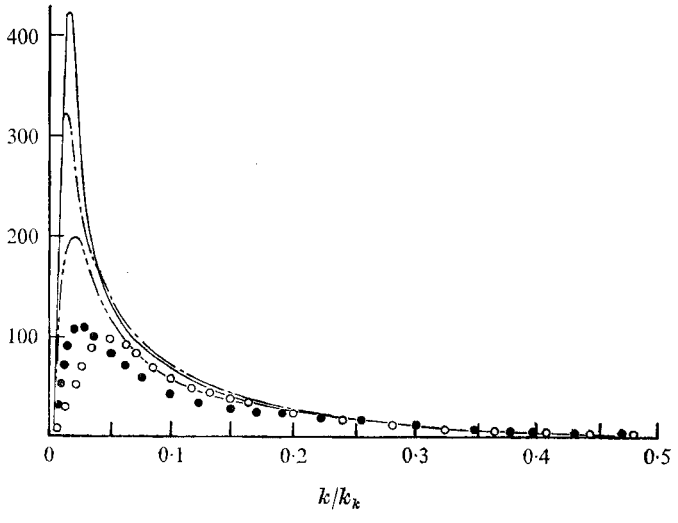

FIGURE 11. Normalized three-dimensional temperature and velocity spectra. $k_K E_\theta(k)/\theta_K^2$: ●, present results. $k_K E_u(k)/v_K^2$: ○, present results; ——, Uberoi, $x/M = 48$; — · —; Uberoi, $x/M = 72$; — · · —, Van Atta & Chen (1969).

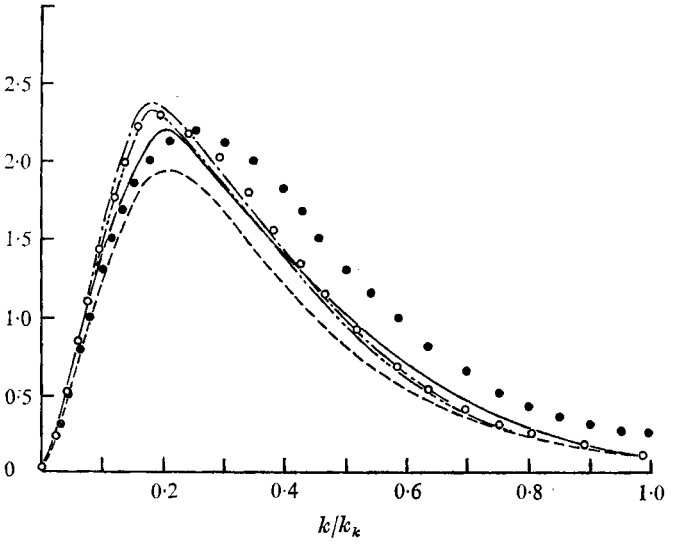

FIGURE 12. Normalized three-dimensional temperature and velocity dissipation spectra. $2\nu_\theta k^2 E_\theta/v_K\theta_K^2$: ●, present results. $2\nu k^2 E_u/v_K^2$: ○, present results; ——, Uberoi, $x/M = 48$; — - - —, Uberoi, $x/M = 72$; —·—, Uberoi, $x/M = 110$; – – – –, Van Atta & Chen (1969).

the maximum values of the kinetic energy spectra are somewhat larger than those reported in I and II, but the values of k/k_k for maximum dissipation are in close agreement. The dissipation spectra, which emphasize the higher wavenumbers, are in very good agreement with those of Uberoi (1963) over the entire range of wavenumbers.

The rates of change of energy spectra $\partial E_n/\partial t$ and $\partial E_\theta/\partial t$ were determined from the relations

$$\frac{\partial E_n}{\partial t} = U\frac{\partial E_n}{\partial x} = -k\frac{\partial}{\partial k}\left(\frac{\partial \phi_{nn}}{\partial t}\right) = -\left(\frac{\partial \phi_{nn}}{\partial t}\right)\frac{\partial \ln(\partial \phi_{nn}/\partial t)}{\partial \ln k}.$$

The last expression is essentially the same as that in the procedure adopted in I and II. Here we have used the average:

$$\frac{\partial E_n}{\partial t} = \frac{1}{2}\left(U\frac{\partial E_n}{\partial x} - \alpha_n(k)\frac{\partial \ln \alpha_n(k)}{\partial \ln k}\right),$$

where $\alpha_n(k) = \partial \phi_{nn}/\partial t = U\partial \phi_{nn}/\partial x$ is the total one-dimensional energy decay. The normalized results for $\partial \phi_{ii}/\partial t$ and $\partial \phi_{\theta\theta}/\partial t$, as well as a comparison of ϕ_{ii} with the results of II are given in figure 13.

The present data for $\partial E_n/\partial t$ are compared with those reported in I and II in figure 14. They are all in fairly good agreement for large wavenumbers, as would be expected for the locally isotropic range of wavenumbers.

Energy transfer spectra

The normalized one-dimensional energy transfer spectra $L_n(k)$ are shown in figure 15. As shown in figures 16 and 17, the corresponding measured triple correlations $R(u\theta, \theta) = \langle u(t)\,\theta(t)\,\theta(t+\tau)\rangle/u'\theta'^2$ and $R(u^2, u) = \langle u^2(t)\,u(t+\tau)\rangle/u'^3$ are

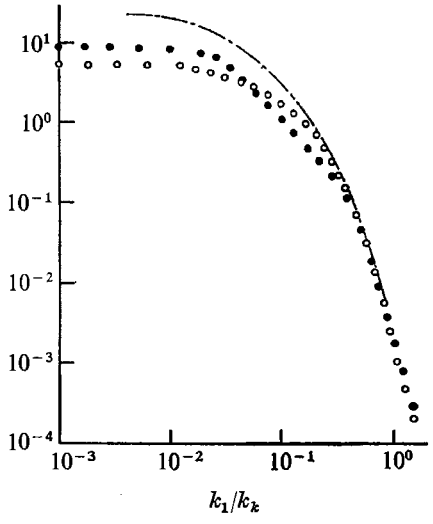

FIGURE 13

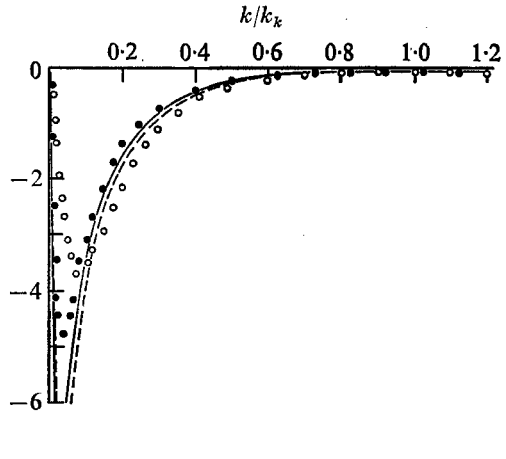

FIGURE 14

FIGURE 13. Decay rate of one-dimensional temperature and velocity spectra. $-(\partial\phi_{\theta\theta}/\partial t)/v_K\theta_K^2$: ●, present results. $-(\partial\phi_{ii}/\partial t)/v_K^3$: ○, present results; —·—; Van Atta & Chen (1969).

FIGURE 14. Decay rate of three-dimensional temperature and velocity spectra. $(\partial E_\theta/\partial t)/\theta_K^2 v_K$: ●, present results. $(\partial E_u/\partial t)/v_K^3$: ○, present results;——, Uberoi; —·—, Van Atta & Chen (1969).

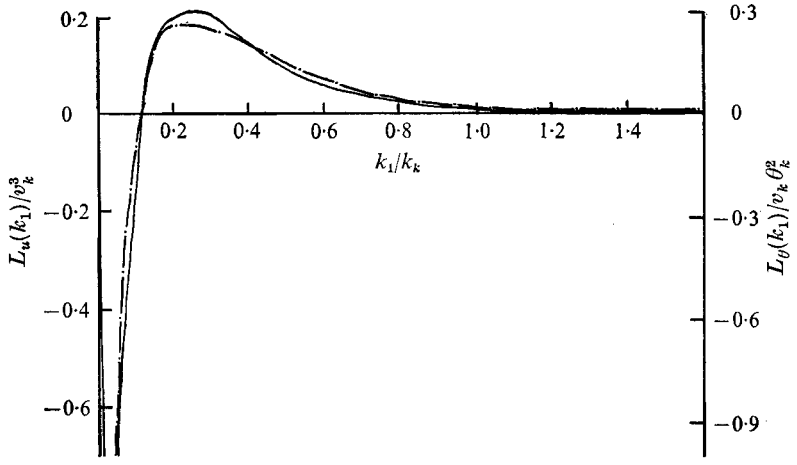

FIGURE 15. One-dimensional transfer spectra of kinetic energy and temperature fluctuations. ——, $L_u(k_1)/v_K^3$; —·—, $L_\theta(k_1)/v_K\theta_K^2$.

nearly antisymmetrical functions of $U\tau/M$. These results indicate that the assumption of isotropy appears reasonably accurate for the triple correlations $R(u\theta, \theta)$ and $R(u^2, u)$, which are the physical space counterparts of the measurable one-dimensional energy transfer functions $L_\theta(k)$ and $L_u(k)$, from which the three-dimensional energy transfer spectra $T_\theta(k)$ and $T_u(k)$ may be determined.

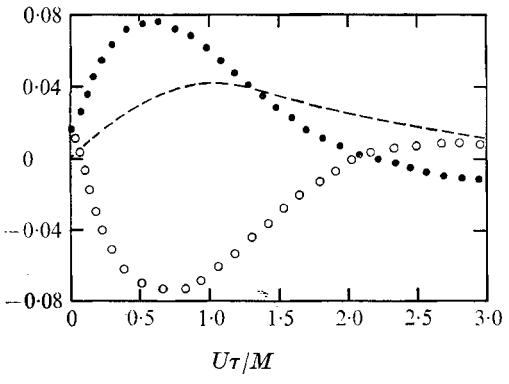

FIGURE 16

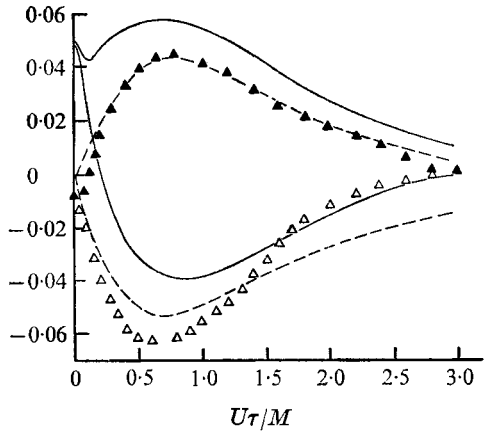

FIGURE 17

FIGURE 16. Third-order mixed correlations of velocity and temperature fluctuations. $R(u\theta, \theta)$: ●, present results. $R(\theta, u\theta)$: ○, present results; ---, Mills *et al.*

FIGURE 17. Triple correlations of u. $R(u^2, u)$: ▲, present results; $R(u, u^2)$: △, present results; ——, Frenkiel & Klebanoff; ---, Van Atta & Chen (1969).

Also shown for comparison in figure 16 is the measured temperature–velocity triple correlation of Mills *et al.* at $x/M = 32$. Their triple correlation has a maximum value about half as large as ours. Attempts to rationalize this difference were impeded by the fact that the measurement of Mills *et al.* was complicated by a large number of isotropic assumptions about unmeasured correlations, a strong dependence of their mixed correlation on the triple velocity correlation, which had to be subtracted from other measured quantities to obtain $R(\theta, u\theta)$, and their operational difficulties associated with matching of hot-wire sensitivities. Another difference is that we measured a two-point time correlation with the sensors at a single spatial location, while Mills *et al.* measured a two-point spatial correlation using a spatial separation of two wires. Useful speculation on the cause of the differences thus appears very difficult at this time.

The three-dimensional energy transfer spectra $T_n(k)$ were directly measured using the method described in § 5 and were also indirectly obtained by summing the experimentally measured $\partial E_n/\partial t$ and $2\nu k^2 E_n(k)$, assuming the validity of the isotropic relation

$$\partial E_n(k)/\partial t = T_n(k) - 2\nu_n k^2 E_n(k). \tag{40}$$

The directly measured $T_n(k)$ for temperature and velocity, normalized with Kolmogorov scaling, are compared with those obtained by using the indirect method in figures 18 and 19. These comparisons may be used to estimate the extent of the validity of the isotropic relation (40) for the present heated-grid turbulence. The directly measured transfer spectra $T_n(k)$ and those obtained from (40) are in good agreement with each other for nearly the entire wavenumber range, except at low wavenumbers ($k/k_k < 0{\cdot}2$) and very large wavenumbers ($k/k_k > 1{\cdot}4$). The large inconsistency at low wavenumbers $k/k_k < 0{\cdot}1$ is most certainly due to the inapplicability of the isotropic relations used to derive $E_n(k)$, $\partial E_n/\partial t$ and $T_n(k)$ from the measured one-dimensional spectra at

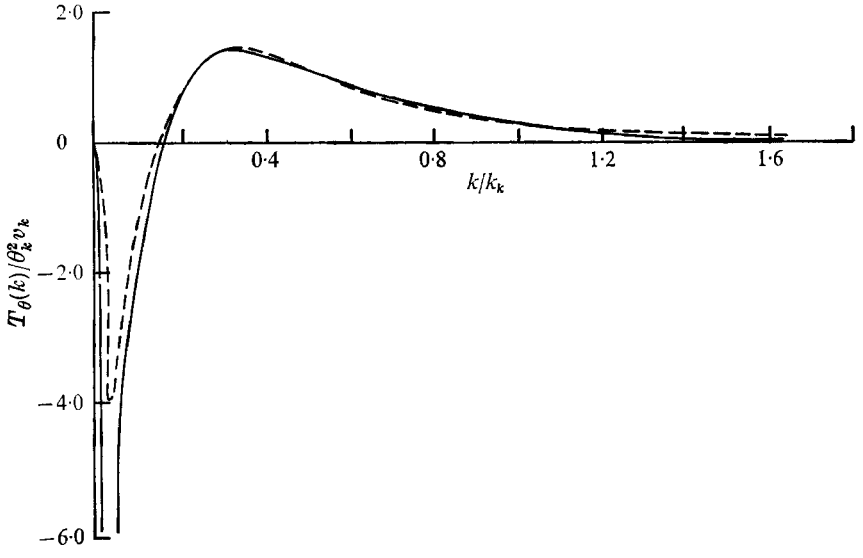

FIGURE 18. Three-dimensional transfer spectra of temperature fluctuations. ——, directly measured $T_\theta(k)$; – – –, $(\partial E_\theta/\partial t) + 2\nu_\theta k^2 E_\theta$.

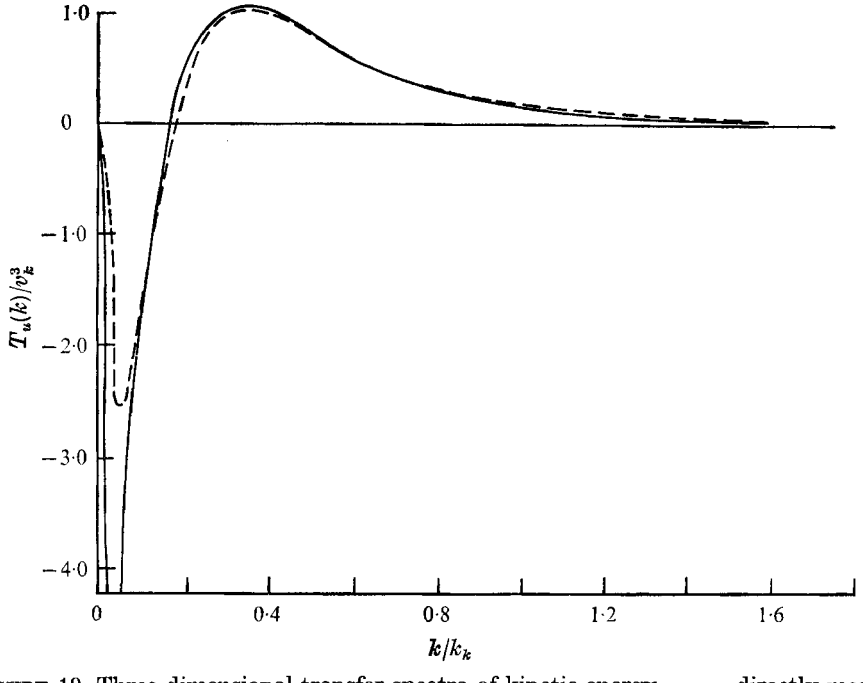

FIGURE 19. Three-dimensional transfer spectra of kinetic energy. ——, directly measured $T_u(k)$; – – – $(\partial E_u/\partial t) + 2\nu k^2 E_u$.

low wavenumbers. The discrepancy at high wavenumbers is probably due to noise generated by uncertainty in the calibration curve fits, which will increase the measured values of $E_n(k)$, and may very well account for the fact that the sum $\partial E_n/\partial t + 2\nu_n k^2 E_n$ is larger than the directly measured $T_n(k)$. Thus, we may conclude that the present heated-grid-generated turbulence is closely

locally isotropic for both temperature and velocity fields for $k/k_k > 0{\cdot}2$. Van Atta & Chen found somewhat better agreement in this respect, but this is probably due to the fact that they measured velocity fluctuations only, for which the noise problem is less severe than for combined temperature and velocity measurements. For $k/k_k < 0{\cdot}16$, the net energy transfer at any given wavenumber k is negative, and for $k/k_k > 0{\cdot}16$ the net transfer is positive. A broad maximum in the transfer spectra for temperature and velocity occurs in the neighbourhood of $k/k_k = 0{\cdot}35$, similar to the results of II. The region $0{\cdot}05 < k/k_k < 0{\cdot}1$, where the measured transfer spectra have large negative values, is of less significance since the turbulence is not locally isotropic for such low wavenumbers and use of the isotropic relations to derive $T_n(k)$ probably produces inaccurate results. Also, the rapid change of $L_n(k)$ in the neighbourhood of $k/k_k = 0{\cdot}08$ may produce unacceptably large uncertainties in the differentiation and hence in $T_n(k)$. Therefore, these large negative values of $T_n(k)$ are not presented in the figures. Because of these difficulties at low wavenumbers the measured transfer functions do not satisfy the zero integral condition of isotropic theory,

$$\int_0^\infty T(k,t)\,dk = 0,$$

as discussed in some detail by Van Atta & Chen (1969). For the present data, the positive contribution of $T_0(k)$ to the integral is roughly 50 % larger than the negative contribution, while the negative contribution from $T_u(k)$ is roughly 10 % greater than the positive one.

The occurrence of only a single value of k where $T_n(k) \simeq 0$, instead of an extended region of k for which $T_n(k) \simeq 0$, may be considered as direct evidence for the non-existence of an inertial–convective subrange, or an inertial subrange in the present flow field. Similar results were obtained in I and II.

The directly measured $T_u(k)$ are compared with those reported in I and II in figure 20. Except at low wavenumbers, the present $T_u(k)$ are in fairly good agreement with those of Uberoi for nearly the entire range of wavenumbers and slightly different from those of Van Atta & Chen at moderate wavenumbers. All are in very good agreement at larger wavenumbers, where the data represent the universal energy transfer spectrum.

Comparison of measured $T_\theta(k)$ with hypotheses

In studying the problem of spectral transfer of kinetic energy, various investigators have proposed hypotheses relating $T_u(k)$ with $E_u(k)$. Some (Obukov 1949; Corrsin 1951) have pointed out that it may be possible to make similar postulates for temperature fluctuations mixed by turbulence, since the temperature transfer mechanism is essentially determined by the same mechanism. Details of the extension of several of these hypotheses to the scalar case are given in the appendix.

One should keep in mind that all these theoretical predictions are essentially conjecture, and that a considerably more satisfactory type of theoretical comparison would be to compare the measured results with more rigorous calculations, based on the Navier–Stokes equations, which do not involve arbitrary

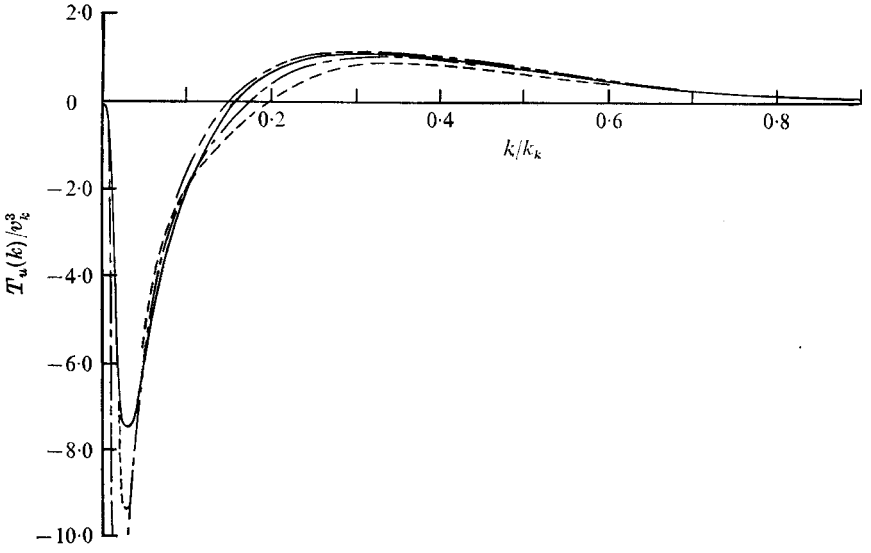

FIGURE 20. Comparison of the measured velocity transfer spectra with previous measurements. ——, present measurements; – – –, Van Atta & Chen (1969). Uberoi: —·—, $x/M = 48$; —··—, $x/M = 72$.

constants. For the case of spectral kinetic energy transfer, calculations of this nature by Kraichnan (1964) using the direct-interaction hypothesis were found in II to be in good agreement with the measured $T_u(k)$, and it is most desirable at this point that theoretical calculations of this type be attempted for the scalar case.

The measured $E_u(k)$ and $E_\theta(k)$ were used to calculate transfer spectra $T_\theta(k)$ according to the extended hypotheses and the results are compared with the measured $T_\theta(k)$ in figures 21 and 22. The universal constant α in each hypothesis, except that of Onsager and Corrsin, can assume a wide range of values depending on the region of k over which the prediction is made to fit the measurements. This is a major disadvantage of these theories. Of course, none of them fits the low wavenumber region of the data. For the Kovasznay–Onsager hypothesis no values for α can be found that will produce a good fit to the data. Heisenberg's theory fits the data for large wavenumbers fairly well by using $\alpha = 0{\cdot}6$. Uberoi and Van Atta & Chen found similar agreement with Heisenberg's hypothesis for the velocity field, with $\alpha = 0{\cdot}2$ and $0{\cdot}25$, respectively. The expression given by Onsager and Corrsin fits the high wavenumber data best if we choose $\alpha = 0{\cdot}5$. The expression contains no unknown constants, other than the 'Obukhov–Corrsin constant', $K_{\theta,3}$ ($\alpha \equiv 1/K_{\theta,3}$). Referring to table 1, the value of α obtained from fitting the measured transfer function is roughly one third of the value obtained from $K_{\theta,3}$. Similar behaviour of $\alpha \simeq (2K_3)^{-1}$ was found by Van Atta & Chen for the velocity field, where K_3 is the three-dimensional Kolmogorov spectral constant for velocity. As shown in figure 22, the modified version of the Obukov hypothesis produces fairly good agreement at high wavenumbers, but increases the discrepancy at low wavenumbers, while neither curve due to von Kármán ($l = m = 0$, $n = \frac{1}{2}$; $l = n = \frac{1}{2}$, $m = 0$) fits the data.

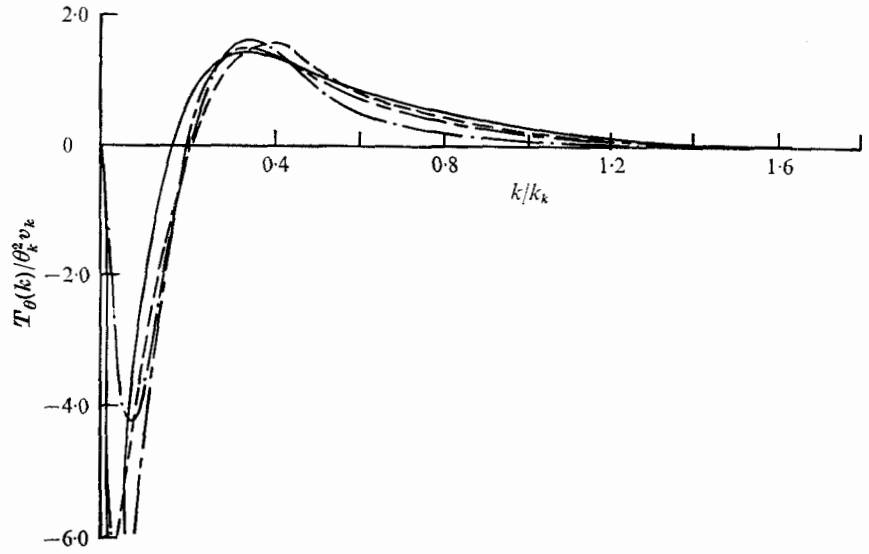

FIGURE 21. Comparison of the temperature transfer spectrum with $T_\theta(k)$ computed from measured $E_u(k)$ and $E_\theta(k)$ using various hypotheses. ——, directly measured T_θ; — · —, Onsager–Corrsin, $\alpha = 0{\cdot}5$; – – –, Heisenberg, $\alpha = 0{\cdot}6$; — · —, Kovasznay–Onsager, $\alpha = 0{\cdot}3$.

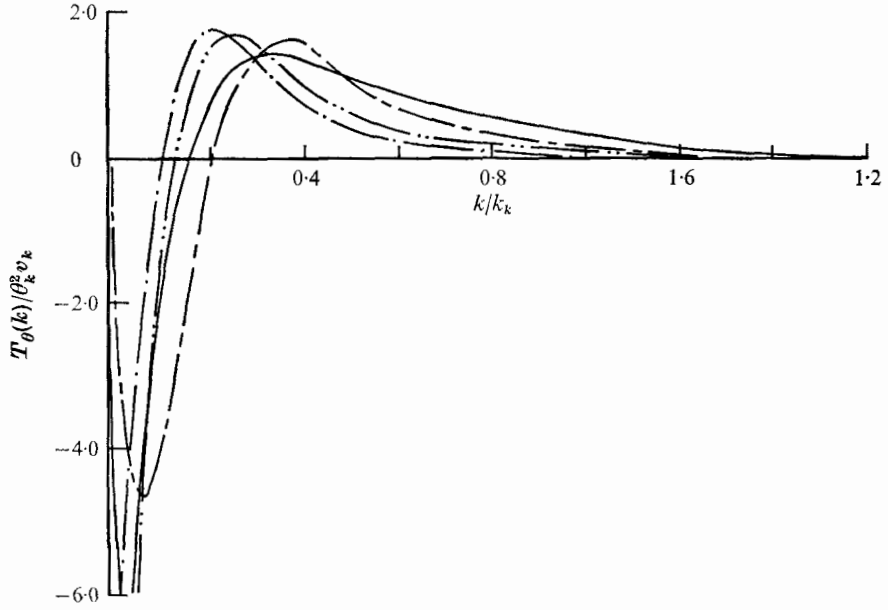

FIGURE 22. Comparison of the temperature transfer spectrum with $T_\theta(k)$ computed from measured $T_u(k)$ and $E_\theta(k)$ using various hypotheses. ——, directly measured $T_\theta(k)$; — · —, modified Obukov, $\alpha = 0{\cdot}3$; — · —, von Kármán, $\alpha = 0{\cdot}35$; — · · —, von Kármán, $\alpha = 0{\cdot}2$.

7. Summary and conclusions

For locally isotropic, homogeneous fluid turbulence, the imaginary part of the cross-spectrum $S_{1n,n}(k_1)$, which is needed to obtain the spectral transfer function $T_n(k)$ for either the kinetic energy or a passive scalar property, can be obtained in several ways: by integration of the imaginary part of a particular one-dimensional bispectrum, from the Fourier transform of a particular two-point triple correlation, or by a direct cross-spectrum estimate. The last method is the most direct one for obtaining T_n, and was used to determine experimentally the spectral transfer functions $T_n(k)$ for velocity and temperature fluctuations in heated-grid turbulence.

For both the temperature and velocity fields, the measured spectral transfer functions are adequately described by the spectral energy balance equations for isotropic turbulence for $k/k_k \geqslant 0{\cdot}2$. The measured velocity transfer spectra are generally consistent with those obtained by Uberoi and Van Atta & Chen, and at large wavenumbers, in the viscous range, all these transfer spectra are universally similar.

Among the various physical hypotheses for spectral transfer, those of Heisenberg, and Onsager and Corrsin produce the best fit to the measured temperature transfer spectra. Direct calculations for the temperature field in decaying isotropic turbulence would furnish a more useful comparison than the physical hypotheses, and it is hoped that these will soon become available.

We thank Dr Paavo Sepri for his help in the laboratory. This work was supported by the Advanced Research Projects Agency of the Department of Defense and was monitored by the U.S. Army Research Office-Durham, Box CM, Duke Station, Durham, North Carolina 27706, under Contract DA-31-124-ARO-D-257 and by the U.S. National Science Foundation under Grant GK-33799. Their support is much appreciated. The paper is adapted from part of Yeh (1971).

Appendix. Hypotheses for spectral transfer

Heisenberg's hypothesis

Corrsin (1951) has extended Heisenberg's (1948) hypothesis to scalar quantities and assumed that the scalar transfer is due to the small eddies acting on the large ones to produce a kind of turbulent diffusion.

Taking

$$\int_k^\infty T_\theta(k)\,dk = 2\epsilon_t(k)\int_0^k k^2 E_\theta\,dk,$$

where $\epsilon_t(k)$ is the turbulent diffusivity caused by the small eddies, dimensional considerations suggest that

$$\epsilon_t(k) = \alpha\int_k^\infty (E_u/k^3)^{\frac{1}{2}}\,dk.$$

Thus,

$$\int_k^\infty T_\theta(k)\,dk = 2\alpha\left[\int_k^\infty (E_u/k^3)^{\frac{1}{2}}\,dk\right]\left[\int_0^k k^2 E_\theta\,dk\right], \tag{A 1}$$

and this gives

$$T_\theta(k) = 2\alpha\left\{(E_u/k^3)^{\frac{1}{2}}\int_0^k k^2 E_\theta\, dk - k^2 E_\theta \int_k^\infty (E_u/k^3)^{\frac{1}{2}}\, dk\right\}. \tag{A 2}$$

Onsager–Corrsin hypothesis

In a variation on a previous theme of Onsager (1949) and Corrsin (1964), Pao (1965) assumed that $\sigma(k)$, the rate at which scalar spectral elements are transferred to a larger wavenumber k, is dependent on ϵ_u and k only. Dimensional reasoning gives $\sigma(k) = \alpha\epsilon_u^{\frac{1}{3}}k^{\frac{1}{3}}$. Thus the scalar spectral flux across k is

$$\int_k^\infty T_\theta(k)\, dk = \sigma(k)\, E_\theta = \alpha\epsilon_u^{\frac{1}{3}}k^{\frac{1}{3}}E_\theta, \tag{A 3}$$

and this gives

$$T_\theta(k) = -\alpha\epsilon_u^{\frac{1}{3}}k^{\frac{2}{3}}E_\theta(\tfrac{5}{3} + d\ln E_\theta/d\ln k). \tag{A 4}$$

Modified Obukov hypothesis

Obukov's (1941) original hypothesis leads to a physically impossible form for the spectrum, and the integral of the transfer function falls to zero at a value of k where the spectrum is finite (Batchelor 1953; Ellison 1962). This problem can be avoided by using Ellison's modification of Obukov's theory, namely, that the fluctuating stress is produced only by eddies in the neighbourhood of k and not by all eddies equally, and is taken to be proportional to $k(E_u E_\theta)^{\frac{1}{2}}$. Thus, we have

$$\int_k^\infty T_\theta(k)\, dk = \alpha\left[2\int_0^k k^2 E_\theta\, dk\right]^{\frac{1}{2}} k(E_u E_\theta)^{\frac{1}{2}} \tag{A 5}$$

and

$$T_\theta(k) = -\alpha(E_u E_\theta)^{\frac{1}{2}}\left(1 + \frac{k^2 E_\theta}{A^2} + \frac{1}{2}\frac{d\ln(E_u E_\theta)}{d\ln k}\right), \tag{A 6}$$

where

$$A(k) = \left[2\int_0^k k^2 E_\theta\, dk\right]^{\frac{1}{2}}.$$

Kovasznay–Onsager hypothesis

Corrsin (1961) has followed Onsager's hypothesis (1945, 1949), which is exactly equivalent to the Kovasznay (1948) hypothesis, and assumed that the scalar spectral flux depends on the spectra E_θ and E_u and wavenumber k only, and not on ν and ν_θ. Thus, the only possible dimensional form for the scalar transfer function is

$$\int_k^\infty T_\theta(k)\, dk = \alpha E_\theta E_u^{\frac{1}{2}}k^{\frac{1}{2}}, \tag{A 7}$$

which gives

$$T_\theta(k) = -\alpha E_\theta E_u^{\frac{1}{2}}k^{\frac{1}{2}}\left[2{\cdot}5 + \frac{d\ln(E_\theta E_u^{\frac{1}{2}})}{d\ln k}\right]. \tag{A 8}$$

Von Kármán's hypothesis

A general expression for scalar spectral flux following von Kármán's postulates (1948) is written as

$$\int_k^\infty T_\theta(k)\, dk = 2\alpha\left[\int_0^k E_\theta^l E_u^m k^n\, dk\right]\left[\int_k^\infty E_\theta^{1-l}E_u^{0{\cdot}5-m}k^{0{\cdot}5-n}\, dk\right]. \tag{A 9}$$

For $l = m = 0$ and $n = \frac{1}{2}$, one obtains a modified Kovasznay–Onsager expression, and for $l = n = \frac{1}{2}$ and $m = 0$, a modified Obukov expression. For $l = 1$, $m = 0$ and $n = 2$, one obtains the Heisenberg hypothesis.

REFERENCES

BATCHELOR, G. K. 1953 *The Theory of Homogeneous Turbulence*. Cambridge University Press.

BATCHELOR, G. K. 1959 *J. Fluid Mech.* **5**, 113.

BATCHLEOR, G. K. 1967 *An Introduction to Fluid Dynamics*. Cambridge University Press.

BRILLINGER, R. R. 1965 *Ann. Math. Statist.* **36**, 1351.

COMTE-BELLOT, G. & CORRSIN, S. 1971 *J. Fluid Mech.* **48**, 273.

COOLEY, J. W. & TUKEY, J. W. 1965 *Math. Comp.* **19**, 297.

CORRSIN, S. 1947 *Rev. Sci. Inst.* **18**, 469.

CORRSIN, S. 1949 *N.A.C.A. Tech. Note*, no. 1864.

CORRSIN, S. 1951 *J. Appl. Phys.* **22**, 469.

CORRSIN, S. 1961 *J. Fluid. Mech.* **11**, 407.

CORRSIN, S. 1964 *Phys. Fluids*, **7**, 1156.

CORRSIN, S. & UBEROI, M. S. 1951 *N.A.C.A. Rep.* no. 1040.

ELLISON, T. H. 1962 *Mécanique de la Turbulence* p. 113. Paris: C.N.R.S.

FRENKIEL, F. N. & KLEBANOFF, P. S. 1967 *Phys. Fluids*, **10**, 507.

GIBSON, C. H. & SCHWARZ, W. H. 1963 *J. Fluid Mech.* **16**, 357.

HAUBRICH, R. A. 1965 *J. Geophys. Res.* **70**, 1415.

HEISENBERG, W. 1948 *Proc. Roy. Soc.* A **195**, 402.

HINZE, J. O. 1959 *Turbulence*. McGraw-Hill.

KIDRON, I. 1966 *DISA Inf.* **4**, 25.

KISTLER, A. L., O'BRIEN, V. & CORRSIN, S. 1956 *J. Aero. Sci.* **96.**

KOVASZNAY, L. S. G. 1948 *J. Aero. Soc.* **15**, 745.

KRAICHNAN, R. 1964 *Phys. Fluids*, **7**, 1030.

LIN, C. C. 1953 *Quart. Appl. Math.* **10**, 295.

LUMLEY, J. L. 1965 *Phys. Fluids*, **8**, 1056.

MILLS, R. R., KISTLER, A. L., O'BRIEN, V. & CORRSIN, S. 1958 *N.A.C.A. Tech. Note.* no. 4288.

MONIN, A. S. & YAGLOM, A. M. 1967 *Statistical Hydrodynamics. Part* 2, *Mechanics of Turbulence* (in Russian). Moscow: Science Publishers.

OBUKOV, A. M. 1941 *C. r. Acad. Sci. U.S.S.R.* **32**, 19.

OBUKOV, A. M. 1949 *Izv. Akad. Nauk.* **13**, 58.

ONSAGER, L. 1945 *Phys. Rev.* **68**, 286.

ONSAGER, L. 1949 *Nuovo Cimento, Suppl.* **6**, 279.

PAO, Y. H. 1965 *Phys. Fluids*, **8**, 1063.

ROBERTSON, H. P. 1940 *Proc. Camb. Phil. Soc.* **36**, 209.

ROSENBLATT, M. & VAN NESS, J. W. 1965 *Ann. Math. Statist.* **36**, 1120.

STEWART, R. W. 1951 *Proc. Camb. Phil. Soc.* **47**, 146.

STEWART, R. W. & TOWNSEND, A. A. 1951 *Phil. Trans.* A **243**, 359.

TOWNSEND, A. A. 1947 *Proc. Camb. Phil. Soc.* **44**, 560.

UBEROI, M. S. 1963 *Phys. Fluids*, **6**, 1048.

UBEROI, M. S. & CORRSIN, S. 1953 *N.A.C.A. Rep.* no. 1142.

VAN ATTA, C. W. & CHEN, W. Y. 1968 *J. Fluid Mech.* **34**, 497.

VAN ATTA, C. W. & CHEN, W. Y. 1969 *J. Fluid Mech.* **38**, 743.

VAN ATTA, C. W. & YEH, T. T. 1970 *J. Fluid Mech.* **41**, 169.

VON KÁRMÁN, T. 1948 *Proc. Natn. Acad. Sci.* **34**, 530.

YEH, T. T. 1971 Ph.D. thesis, University of California, San Diego.